ASEAN
Journal of Scientific and Technological Reports
Online ISSN:2773-8752

Research article

# Efficient Photodegradation of Biebrich Scarlet in Water by CuFe-LDH Decorated with Potential Photocatalysts

**Krongkhwun Chaiyapat[1, 9], Pruettiphong Phiromrak[2, 9], Krongnet Sangthong[3, 10], Phitchayaphak Saenplee[4, 10], Panita Sumanatrakul[5], Nantharat Phruksaphithak[6], Akkanee Pewhom[7], and Sonchai Intachai[8, 10*]**

[1] Faculty of Science and Digital Innovation, Thaksin University, Phatthalung, 93210, Thailand
[2] Faculty of Science and Digital Innovation, Thaksin University, Phatthalung, 93210, Thailand
[3] Faculty of Science and Digital Innovation, Thaksin University, Phatthalung, 93210, Thailand
[4] Faculty of Science and Digital Innovation, Thaksin University, Phatthalung, 93210, Thailand
[5] Faculty of Engineering, Thaksin University, Phatthalung, 93210, Thailand
[6] Faculty of Science and Digital Innovation, Thaksin University, Phatthalung, 93210, Thailand
[7] Faculty of Science and Digital Innovation, Thaksin University, Phatthalung, 93210, Thailand
[8] Faculty of Science and Digital Innovation, Thaksin University, Phatthalung, 93210, Thailand
[9] Science Classrooms in University - Affiliated School Project (SCiUS), Paphayompittayakom School, Phatthalung, 93210, Thailand
[10] Innovative Materials Chemistry for Environment Center, Thaksin University, Phatthalung, 93210, Thailand
* Correspondence: sonchai.i@tsu.ac.th

**Citation:**
Chaiyapat, K.; Phiromrak, P.; Sangthong, K.; Saenplee, P.; Sumanatrakul, P.; Phruksaphithak, N.; Pewhom, A.; Intachai, S. Efficient photodegradation of biebrich scarlet in water by CuFe-LDH decorated with potential photocatalysts. *ASEAN J. Sci. Tech. Report.* **2025**, *28*(2), e256514. https://doi.org/10.55164/ajstr.v28i2.256514

**Article history:**
Received: October 30, 2024
Revised: January 17, 2025
Accepted: January 23, 2025
Available online: February 23, 2025

**Abstract:** CuFe-layered double hydroxide (CuFe-LDH) is an environmentally friendly 2D material with positively charged active sites, offering a high ability to remove toxic anionic chemicals in wastewater. In the study, CuFe-LDH was synthesized by the precipitation under magnetic stirring for 12 h, followed by the hydrothermal reaction at 160 °C for 8 h, and utilized as both adsorbent and photocatalyst for eliminating Biebrich Scarlet anions from water. The as-prepared product corresponded to the LDH brucite-like structure with the interlayer nitrate anions and was decorated with FeOOH, $Fe_2O_3$, and CuO. Besides, CuAl-LDH exhibited a large surface area and broad absorption band in the 400–800 nm wavelength range. The product exhibited a high maximum adsorption capacity for removing Biebrich Scarlet in water through the electrostatic interaction and the efficient photocatalytic activity under visible light irradiation for 240 min. The excellent removal efficiency of the toxic species in water was attributed to the combined effects of CuFe-LDH and the semiconducting properties of FeOOH, $Fe_2O_3$, and CuO.

**Keywords:** Layered double hydroxide; Biebrich scarlet; FeOOH; $Fe_2O_3$; CuO

## 1. Introduction

Water is an essential natural resource for all living organisms. Therefore, preserving clean water and purifying wastewater are the most important and challenging. Because many domestic, industrial, and agricultural activities of several dangerous species significantly remained, they were subsequently discharged into natural water resources. Synthetic dye is mostly a vital environmental danger, carcinogen, and irritant [1 - 3], a serious topic of environmental issues that requires an urgent finding of an optimized solution. Biebrich Scarlet is a toxic organic anion of sodium salt in water, and large amounts are used for biological and pathological studies [4, 5].

Recently, dye wastewater treatment has been addressed by many efficient procedures such as chemical, biological, and physical pathways [3 - 5].

However, chemical adsorption [1] and photocatalysis [2] have received much interest in the advantages of fast and reusable activities for degrading dye structures. Especially solid materials gain such merits as high stability for long-term light exposure, large surface area, and visible light response [6 - 8]. Layered double hydroxide (LDH), a two-dimensional layered material, is categorized as an inorganic solid material with large surface area that originated by substituting some divalent metal ($M^{2+}$) sites in the brucite layer by trivalent metal ($M^{3+}$), resulting net positively-charged layer with counterbalancing of interlayer anions ($A^{n-}$), as a typical formula of $[M_{1-x}^{2+}M_x^{3+}(OH)_2](A^{n-})_{x/n}\cdot zH_2O$ [10]. Furthermore, its structure is tunable by varying $M^{2+}$ and $M^{3+}$ as we all select environmentally friendly ions to optimize optical and magnetic features [9, 11]. One of the LDH materials, CuFe-LDH, was obtained much investigation as an efficient adsorbent and photocatalyst for the elimination of anionic dyes from water because of its large surface area and broad spectrum throughout visible light, as well as very low toxicity of $Cu^{2+}$ and $Fe^{3+}$ species [1, 12 - 14]. The preparation method is highly affected by the phase structure, crystallinity, and optical and magnetic properties. Many reports showed that the hydrothermal process, a heat-treating method, offered the higher crystalline LDH, and sometimes the formation of secondary phases of metal oxides conducted by heating two metal ions ($M^{2+}$ and $M^{3+}$) in the presence of $OH^-$ ions [8, 9]. Fortunately, NiO and $Fe_2O_3$ were formed on the NiFe-LDH surface under the hydrothermal method between $Ni^{2+}$ and $Fe^{3+}$ as well as excess $OH^-$ species, which were co-semiconducting photocatalyst on tailoring the photodegradation efficiency of Congo red in water [15]. As a result, the fabrication of CuFe-LDH under the hydrothermally heating of $Cu^{2+}$, $Fe^{3+,}$ and $OH^-$ may generate CuO, $Fe_2O_3$, and/or others, where all are efficient visible light-harvesting photocatalyst on decomposing toxic organic dye in water [2, 15, 16].

The adsorptive and photocatalytic elimination of Biebrich Scarlet in water by CuFe-LDH trapped with visible-light-driven photocatalysts has not been investigated. In this study, CuFe-LDH was prepared using precipitation. Then, the hydrothermal reaction of $Cu^{2+}$, $Fe^{3+,}$ and $OH^-$ was applied as the adsorbent and visible light-driven-photocatalyst on removing Biebrich Scarlet anionic dye from water. Besides, the adsorption kinetic and equilibrium of Biebrich Scarlet were also explored by fitting *pseudo*-first order and *pseudo*-second order profiles, as well as Langmuir and Freundlich models. The photocatalytic performance was verified by the profiles of the kinetic rate constant obtained by following the *pseudo*-first-order reaction and reusability. The present study may provide a valuable procedure for designing a stable adsorbent and photocatalyst for fast and completely purifying dye-contaminated wastewater.

## 2. Materials and Methods

### 2.1 Materials

Iron (III) nitrate hexahydrate ($Fe(NO_3)_3\cdot 6H_2O$) was obtained by KemAus. Copper(II) nitrate trihydrate ($Cu(NO_3)_2\cdot 3H_2O$) was purchased from Carlo Erba Reagenti. Sodium hydroxide (NaOH) and hydrochloric acid solution (conc. HCl solution) were produced by Sigma-Aldrich. Biebrich Scarlet ($C_{22}H_{14}N_4Na_2O_7S_2$) was supplied from Acros. All chemicals are of reagent grade and were used directly without further purification.

### 2.2 Preparation of CuFe-LDH-based adsorbent and photocatalyst

Firstly, the appreciated amount of aqueous solution of NaOH was slightly dropped into the aqueous solution of $Cu(NO_3)_2$ and $Fe(NO_3)_3$ mixture until the pH reached 9.0. The reaction was carried out under magnetic stirring for 12 h, where the molar ratio of $Cu^{2+}$: $Fe^{3+}$ was 3:1 [1]. Then, it was transferred into a hydrothermal reactor, sealed tightly, and placed in an oven at 160°C for 8 h [15]. The resulting precipitate was washed with deionized water several times until the pH was approximately 7 and continually cleaned with ethanol. The solid product was dried at 60 °C for 12 h, then ground into fine powder.

### 2.3 Removal of Biebrich Scarlet from water

The adsorption reaction was conducted by mixing 0.02 g adsorbent and 100 ppm 100 mL dye-wastewater under magnetic stirring in the dark for 60 min. The supernatant was collected every 10 min of reaction time to measure the absorbance at 510 nm using UV-VIS spectrophotometry. After reaching the equilibrium (for 60 min in the dark), the photocatalytic activity (0.005 g photocatalyst in 100 ppm 100 mL wastewater) was further run to completely degrade the dye structure under visible light irradiation (200 W tungsten halogen lamp) at about 25 °C. The supernatant was collected every 30 min of the photocatalytic reaction to measure the absorbance using UV-VIS spectrophotometry. The parameters of adsorption and photocatalysis were determined by following the equations, as shown in Table 1.

### 2.4 Characterization

Various techniques characterized the as-prepared sample and its properties; a powder X-ray diffraction (XRD) pattern was conducted using a PANalytical Empyrean powder diffractometer. Fourier transformed infrared (FT-IR) spectrum was carried out using a Perkin Elmer Spectrum One FT-IR spectrophotometer. The Zeta potential of the sample dispersing in DI water was explored at 25 °C using a Zetasizer (Nano ZS, Malvern, Worcestershire, UK). $N_2$ adsorption-desorption isotherm was performed using Micromeritics ASAP 2010 equipment, and the degassing process was conducted at 120 °C under a vacuum atmosphere for 3 h. The optical property was investigated using a Shimadzu UV-VIS-NIR 3101PC spectrophotometer. The amount of dye in the aqueous solution was determined using a Shimadzu UV-1700 Pharmaspec UV-VIS spectrophotometer.

**Table 1.** Equations for adsorption study and photocatalytic rate constant.

| Parameter | Equation |
|---|---|
| Adsorption efficiency (%) | $(C_0 - C_t)/C_0 \times 100$ |
| Removal efficiency at equilibrium, $q_e$ (mg/g) | $(C_0 - C_e)/m \times V$ |
| Removal efficiency at any time, $q_t$ (mg/g) | $(C_0 - C_t)/m \times V$ |
| *Pseudo*-first order reaction | $\log(q_e - q_t) = \log q_e - k_1 t/2.303$ |
| *Pseudo*-second order reaction | $t/q_t = 1/k_2(q_e)^2 + t/q_e$ |
| Langmuir model | $C_e/q_e = C_e/q_m + 1/K_L q_m$ |
| Freundlich model | $\log q_e = \log k_F + (1/n)\log C_e$ |
| Photocatalytic *pseudo*-first-order reaction | $\ln(C_0/C_t) = k_{app}t$ |

Where "$C_0$, $C_t$, and $C_e$" are the concentration (mg/L) of dye at the initial time, different "t" time, and equilibrium, respectively. $q_t$ and $q_e$ are removal capacity (mg/g) at any time and equilibrium, respectively, m (g) is the mass of the adsorbent, and V (L) is the volume of the dye solution. $k_1$ ($min^{-1}$) and $k_2$ ($g \cdot mg^{-1} \cdot min^{-1}$) are the *pseudo*-first order and *pseudo*-second order rate constant, respectively. $q_m$ (mg/g) is the maximum adsorption capacity, $K_L$ (L/mg) is the Langmuir constant, 1/n is the heterogeneity factor, and $K_F$ ($(mg/g)(L/mg)^{1/n}$) is the Freundlich constant. The $k_{app}$ is the apparent *pseudo*-first-order kinetic rate constant.

## 3. Results and Discussion

### 3.1 Characterization

The obtained product powder was dark brown, attributing to the mixed electronic spectra of $Cu^{2+}$ and $Fe^{3+}$ in various environments, as shown in the inset of Figure 1. Further characterization was conducted using an XRD pattern, which revealed multiple peaks corresponding to different material phases (Figure 1). The diffraction peaks observed at 12.9 and 25.9° match (*003*) and (*006*) reflections (positioning with ∇), corresponding to the brucite-like diffraction pattern due to LDH structure. Taking the $d_{003}$ (6.92 Å) into account by diminishing the layer thickness (4.8 Å), the interlayer distance was 2.12 Å, which was indicative of the intercalation of nitrate anion ($NO_3^-$) [1, 17]. Additionally, there were several XRD peaks from $2\theta = 20$, which were grouped into three materials, where the reflections of (*110*), (*130*), (*111*), (*121*), and (*140*) remarking with ♥ were following α-FeOOH phase [16]. Meanwhile (*220*), (*221*), (*311*), (*400*), (*422*), (*511*) and (*440*) planes (representing with ♦) were according to γ-$Fe_2O_3$ [15], and those of (*110*), (*002*), (*111*), (*112*), (*-202*), (*020*), (*202*), (*-113*), (*-311*) and (*220*) reflections labeling with ♣ were due to CuO particles [2]. The findings could confirm the formation of CuFe-LDH, which is decorated with three impurity phases of FeOOH, $Fe_2O_3$, and CuO on the external surfaces. These secondary phases were fabricated by reacting $Cu^{2+}$ and $Fe^{3+}$ reactive species to the excess OH under heating at 160 °C for 8 h, which might be an effective visible light-harvesting photocatalyst.

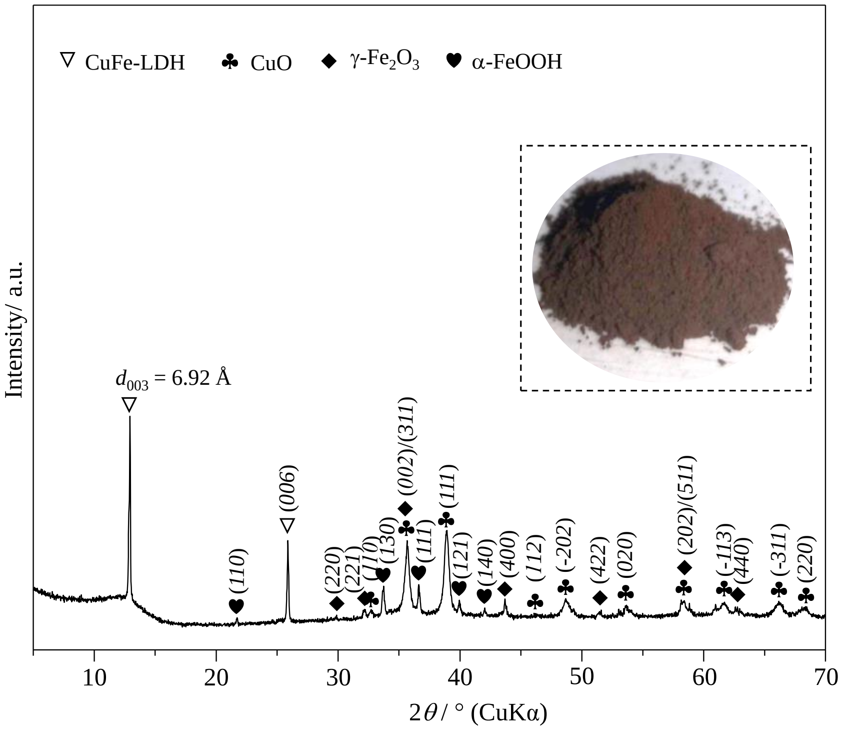

**Figure 1.** XRD pattern of the as-synthesized CuFe-LDH and its powder color (inset).

The functional groups of the product were further analyzed using the FT-IR spectrum, as shown in Figure 2. The infrared bands observed at 3539 and 3398 $cm^{-1}$ due to the stretching vibration modes of O–H bonds of FeOOH and the interlayer $H_2O$ and hydroxide layer of CuFe-LDH; meanwhile, the bending vibration mode due to the adsorbed $H_2O$ observed at 1364 $cm^{-1}$ [10, 11, 16.]. The sharp infrared band appeared at 1333 $cm^{-1}$, corresponding to the vibration of $NO_3^-$ in the interlayer space [1, 17], and two FT-IR bands observed at 1418 and 1046 $cm^{-1}$ were assigned to the interlayer $CO_3^{2-}$ ions derived from the dissolved $CO_2$ in water [1,15]. Below 1000 $cm^{-1}$, the observed FT-IR bands corresponded to the M–O and/or M–O–M bonds, where M is the representative of $Cu^{2+}$ and/or $Fe^{3+}$ for CuFe-LDH, FeOOH, $Fe_2O_3$, and/or CuO that mentioned in the XRD part [4, 12].

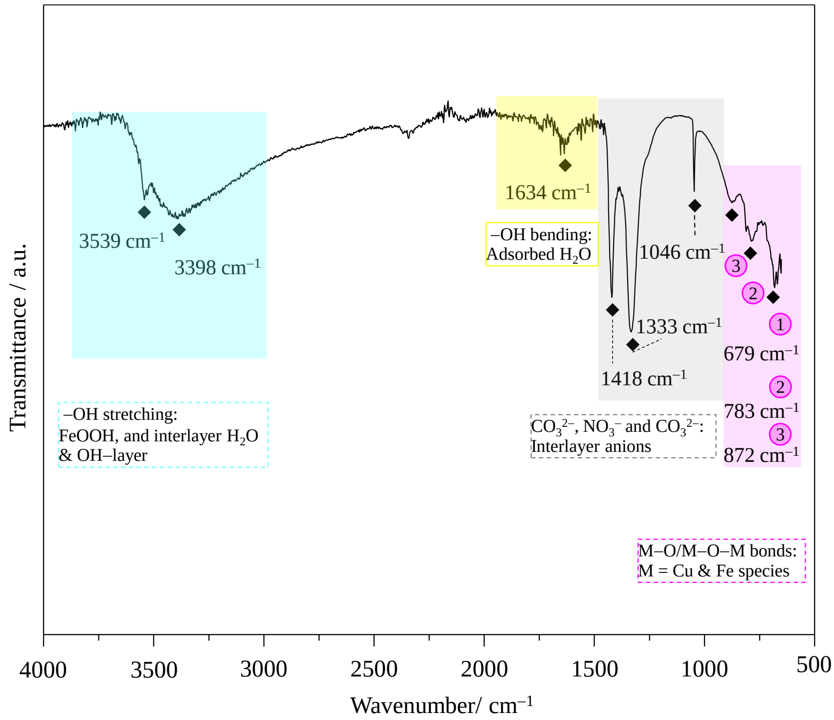

**Figure 2.** FT-IR spectrum of the as-prepared CuFe-LDH material.

The diffuse reflectance absorption spectrum of the product was analyzed to evaluate its optical properties, which exhibited a broad absorption spectrum ranging from 200 to 800 nm. (Figure 3), as the result of the overlapped optical characteristics of CuFe-LDH, FeOOH, $Fe_2O_3$, and CuO [16, 18, 19]. The strong absorption band started from 200 to 385 nm and centered at 350 nm, corresponding to the charge transfer from ligand ($O_{2p}$) to metal ($Cu_{3d}$ and $Fe_{3d}$) [15]. It was noted that the absorption band at the lower energy region overlapped between the d-d transitions due to Cu2+ (d9) in the octahedral crystal field and the defects in FeOOH, $Fe_2O_3$, and CuO semiconductors [15, 20]. Notably, the as-prepared product showed an intense optical response through UV-visible light, which could be applied as an efficient photocatalyst.

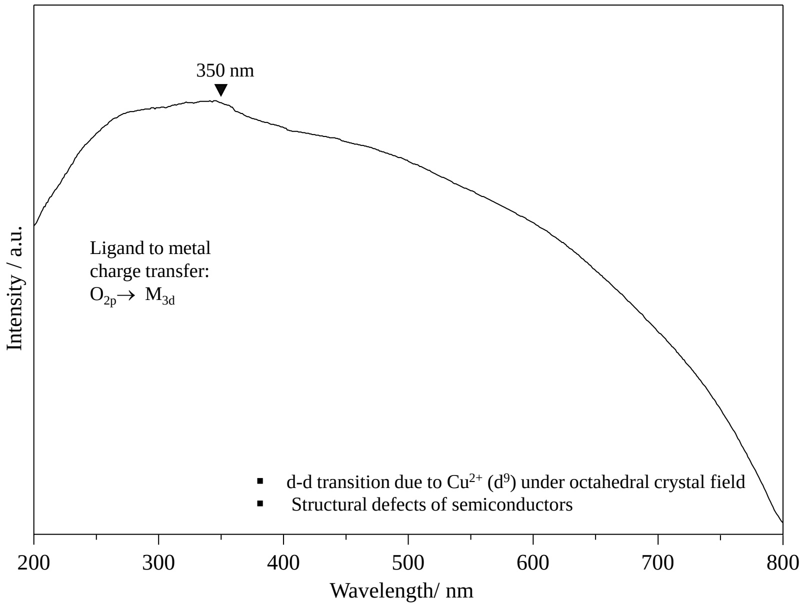

**Figure 3.** Diffuse reflectance absorption spectrum of the as-prepared CuFe-LDH material showing broad absorption from 200 to 800 nm

### 3.2 Adsorption and photocatalysis

The capacity of the product to remove Biebrich Scarlet from water was evaluated through adsorption in the dark and photocatalysis under visible light irradiation. As seen in Figure 4a, the adsorption efficiency of Biebrich Scarlet increased sharply to 43% and 64% within 10 and 20 min, respectively, and gradually rose to 83 % for 60 min at the equilibrium. The adsorption process corresponded to the *pseudo*-second-order reaction, which was dependent on the quantities of dye and adsorbent in the system (Figure 4b, $R^2 = 0.9760$), relative to the *pseudo*-first-order model (Figure 4b, $R^2 = 0.9953$) [10, 11]. By varying the dye concentration, the equilibrium isotherm was linearly plotted. Considering the $R^2$, the adsorption activity was more preferred to the Langmuir profile (Figure 4c, $R^2 = 0.9999$) than that of the Freundlich model (Figure 4d, $R^2 = 0.8856$), which could be indicative of the monolayer coverage [8, 20]. The resulting Langmuir data shows that the product's maximum adsorption capacity (qm) was 520 mg/g. The BET surface area, zeta potential, and pH at the point of zero charge (pHpzc, followed by drift method [8]) were investigated to verify. The product showed a large surface area (67 $m^2/g$), positive zeta potential (+14 mV), and $pH_{pzc} = 8.03$. Without the pH adjustment, the reaction pH was 6.3, which could describe the adsorption of Biebrich Scarlet anions on the positively charged surface of the product via the electrostatic interaction [9]. Based on the corresponding functional groups, the adsorption reaction between the adsorbent (–O and –OH) and adsorbate (–O, –OH and –N, as shown in Figure 4a (inset)) was also driven by hydrogen bonding [10, 11]. These merits of the product promoted the fast and efficient removal of the toxic dye anions in water. The $q_m$ data were depicted in Table 2, indicating that the as-prepared product was an efficient adsorbent in eliminating Biebrich Scarlet in water relative to other adsorbents, which might be due to large surface area and positively-charged active sites.

**Table 2.** Comparation of adsorption and photocatalytic capacities on removing Biebrich Scarlet in water.

| Material | BET surface area / $m^2/g$ | pH | $pH_{pzc}$ | Maximum adsorption capacity ($q_m$) / mg/g | Photocatalytic kinetic constant ($K_{app}$) / $min^{-1}$ | Ref. |
|---|---|---|---|---|---|---|
| CuFe-LDH decorated with FeOOH, $Fe_2O_3$ and CuO | 67 | 6.3 | 8.03 | 520 | 0.0188 (VIS) | Present work |
| CLDH | 131.7 | 5 | 12 | 98.33 | - | [4] |
| NiO-M | 44.21 | - | - | 22.46 | - | [22] |
| NiO-C | 26.895 | - | - | 19.28 | - | [22] |
| ZnO | - | 10 | - | - | 0.3591 (UV) | [21] |
| ZnO-$SnO_2$ | - | 6 | 7 | - | 0.0548 (UV) | [23] |

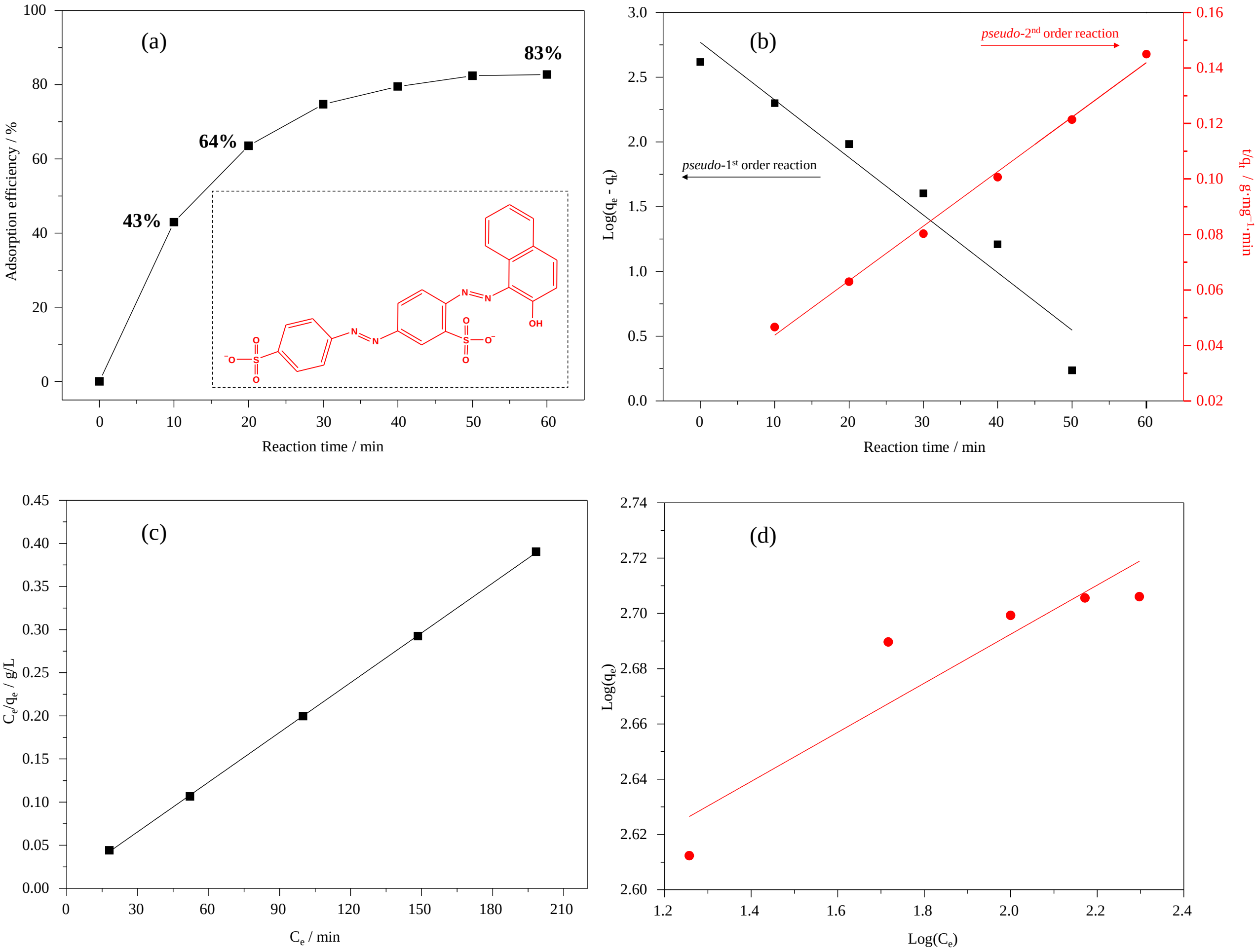

**Figure 4.** Removal profiles of Biebrich Scarlet in water (a) adsorption efficiency and (inset) structure of Biebrich Scarlet, (b) kinetic plots, (c) Langmuir isotherm, and (d) Freundlich isotherm.

The photocatalytic activity was carried out using a 0.005 g photocatalyst to remove the dye in water (100 ppm 100 mL) under magnetic stirring and illuminating visible light for over 240 min. In Figure 5a, after adsorption equilibrium, the amounts of Biebrich Scarlet were largely photodegraded (69 %) within just 60 min of visible light irradiation and slightly photodecomposed up to 100 % within 240 min. In contrast, the photolysis (without photocatalyst) was negligible. The kinetics of the photocatalytic degradation of the dangerous dye in water was fitted by the *pseudo*-first-order equation ($R^2 = 0.9993$) as displayed in Figure 5b, providing the rate constant was 0.0188 $min^{-1}$, showing the fast and efficient dye-photodegradation. The high degradation efficiency may result from the large amounts of dye adsorbed on active sites, enabling rapid degradation through reactive species ($^{\bullet}OH$ and $^{\bullet}O_2^-$) generated by the semiconductors (FeOOH, $Fe_2O_3$, CuO) and LDH (via d-d transitions) [15, 12, 16, 20]. The excited electron and hole were thought to be fast, easily generated, and slowly recombined, transferring through the heterostructure among FeOOH, $Fe_2O_3$, and CuO because of their closely aligned and narrow band gap [12 - 14]. These mechanisms were consistent with other reports on the decomposition of organic dye in water under visible light irradiation. These showed the potential capacity of FeOOH, $Fe_2O_3$, and CuO due to easy electron-hole generation and transportation in the heterojunction structure [21 - 23]. Furthermore, the LDH acted efficiently as the photocatalyst through d-d transition [15, 20]. Considering the rate constant relative to other photocatalysts driven by UV light irradiation [Table 2], the as-prepared product was a potential photocatalyst for degrading Biebrich Scarlet in water under visible light irradiation with notable environmental and economic benefits.

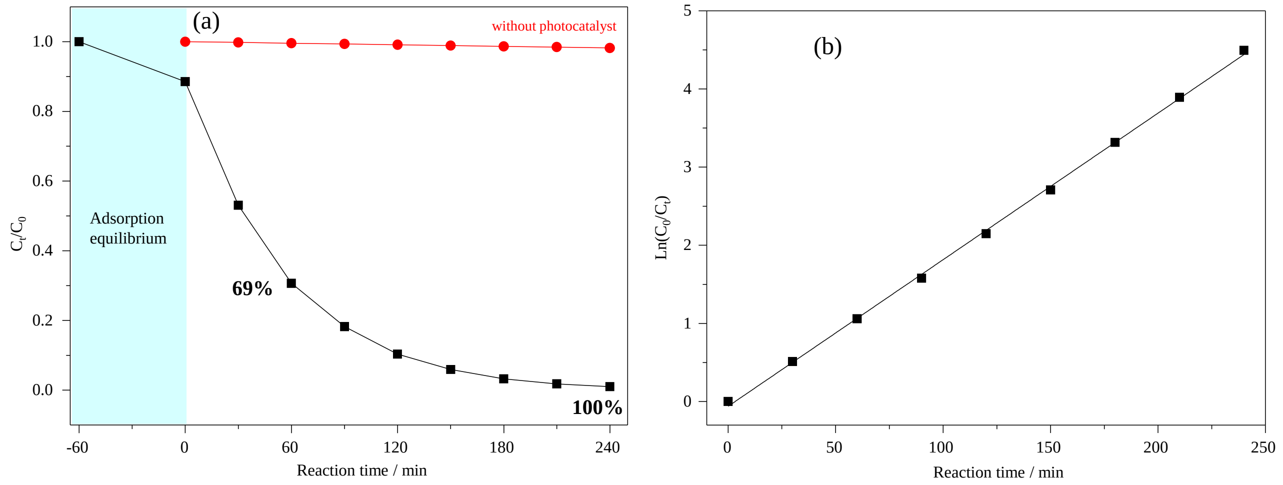

**Figure 5.** Photodegradation of Biebrich Scarlet in water (a) photocatalytic efficiency and (b) kinetic plot.

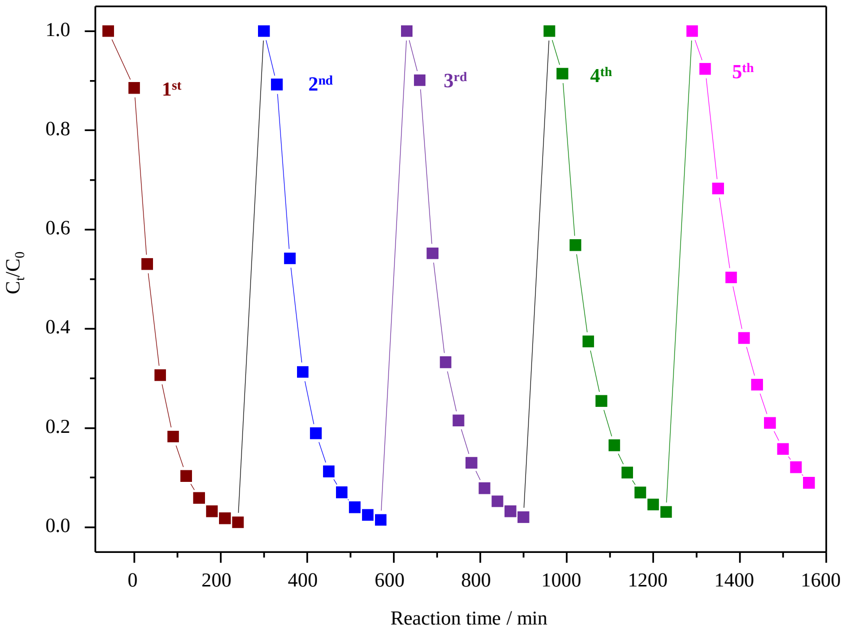

**Figure 6.** Photocatalytic performance of the product on recycling multiple times.

The performance of the obtained photocatalyst was further investigated by the reusability for removing Biebrich Scarlet in water (Figure 5), following the same procedures in the first use. Before reuse, the spent CuFe-LDH decorated with FeOOH, $Fe_2O_3$, and CuO was cleaned by dispersing it in ethanol under vigorous magnetic stirring three times and then ultrasonication for 30 min. Notably, the photocatalytic efficiency decreased slightly by only 9% after 5th reuse cycle. This minor decline was typically attributed to the gradual deterioration of structural, morphological, and optical characteristics [13, 14]. As a result, the as-prepared product was a smart material for eliminating toxic organic dye in water through adsorption and photocatalysis with reusable capacity over multiple cycles. However, further studies will be conducted to verify and describe the photocatalytic activity and the spent product's structural, morphological, and optical changes.

## 4. Conclusions

CuFe-LDH, mixed with FeOOH, $Fe_2O_3$, and CuO, was successfully synthesized using precipitation and hydrothermal methods. The product showed a large surface area (67 $m^2/g$), positively-charged surface (+14 mV), and strong visible light absorption, an efficient adsorbent and visible-light-driven photocatalyst. The maximum adsorption capacity was 520 mg/g for removing Biebrich Scarlet anions in water by the electrostatic and hydrogen-bonding interactions, followed by the *pseudo*-second-order reaction and monolayer coverage. The photocatalyst showed great photocatalytic activity on degrading all Biebrich Scarlet anions in water within 240 min of visible light irradiation with the photocatalytic rate constant of 0.0188 $min^{-1}$. It could be reused up to the 5th cycle without significantly reducing the photocatalytic efficiency. This work provides a precise preparation method for synthesizing multifunctional materials as a promising adsorbent and photocatalyst.

## 5. Acknowledgements

We sincerely acknowledge the scientific instrument support from the Department of Physical Science, Faculty of Science and Digital Innovation, Thaksin University.

**Author Contributions:** Conceptualization; supervision; funding acquisition, S.I.; methodology, K.C. and P.P.; investigation, K.S. and P.S.[2]; writing-original draft preparation, K.C., P.P., and S.I.; writing-review and editing, K.C., P.P., S.I., P.S.[3], N.P. and A.P.

**Funding:** This work was supported by the National Science, Research and Innovation Fund (NSRF), Thaksin University (Research project grant) Fiscal Year 2025, and partially funded by Innovative Materials Chemistry for Environment Center, Thaksin University Research Fund, Thailand.

**Conflicts of Interest:** Declare conflicts of interest or state, "The authors declare no conflict of interest."

## References

[1] Zubair, M.; Aziz, H.A.; Ihsanullah, I.; Ahmad, M.A.; Al-Harthi, M.A. Biochar supported CuFe layered double hydroxide composite as a sustainable adsorbent for efficient removal of anionic azo dye from water. *Environmental Technology & Innovation*, **2021**, *23*, 101614. https://doi.org/10.1016/j.eti.2021.101614

[2] Raizada, P.; Sudhaik, A.; Patial, S.; Hasija, V.; Khan, A.A.P.; Singh, P.; Gautam, S.; Kaur, M.; Nguyen, V.H. Engineering nanostructures of CuO-based photocatalysts for water treatment: Current progress and future challenges. *Arabian Journal of Chemistry*, **2020**, *13*(11), 8424-8457. https://doi.org/10.1016/j.arabjc.2020.06.031

[3] Vo, T.P.; Danaee, S.; Chaiwong, C.; Pham, B.T.; Kim, M.; Kuzhiumparambil, U.; Songsomboon, C.; Pernice, M.; Ngo, H.H.; Ralph, P.J.; Vo, P.H. Microalgae-bacteria consortia for organic pollutants remediation from wastewater: A critical review. *Journal of Environmental Chemical Engineering*, **2024**, 114213. https://doi.org/10.1016/j.jece.2024.114213

[4] Chebli, D.; Bouguettoucha, A.; Reffas, A.; Tiar, C.; Boutahala, M.; Gulyas, H.; Amrane, A. Removal of the anionic dye biebrich scarlet from water by adsorption to calcined and non-calcined Mg–Al layered double hydroxides. *Desalination and Water Treatment*, **2016**, *57*(46), 22061-22073. https://doi.org/10.1080/19443994.2015.1128365

[5] Yadav, L. C.; Jaimini, H.; Meena, R.; Meena, S. Degradation of biebrich scarlet textile dye by using MBIR Dowex-1x8. *Oriental Journal of Chemistry*, **2023**, *39*(4), 942-947. https://doi.org/10.13005/ojc/390416

[6] Poosimma, P.; Ontam, A.; Intachai, S.; Khaorapapong, N.; Ogawa, M. Control of the optical properties of cadmium selenide nanoparticles using magadiite. *Dalton Transactions*, **2018**, *47*, 807-813. https://doi.org/10.1039/C7DT03297H

[7] Suppaso, C.; Pongkan, N.; Intachai, I.; Inchongkol, Y.; Bureekaew, S.; Khaorapapong, N. Tin sulfides and cadmium sulfide mixture in montmorillonite with enhanced visible-light photocatalytic activity. *Applied Clay Science*, **2023**, *241*, 106999. https://doi.org/10.1016/j.clay.2023.106999

[8] Intachai, S.; Tongchoo, P.; Sumanatrakul, P.; Pankam, P.; Khaorapapong, N. Efficient and practical adsorption of mixed anionic dyes in aqueous solution by magnetic NiFe-layered double oxide. *Korean Journal of Chemical Engineering*, **2022**, *39*(10), 2675-2684. https://doi.org/10.1007/s11814-022-1099-y

[9] Intachai, S.; Nakorn, M.N.; Kaewnok, A.; Pankam, P.; Sumanatrakul, P.; Khaorapapong, N. Versatile inorganic adsorbent for efficient and practical removal of hexavalent chromium in water. *Materials Chemistry and Physics*, **2022**, *288*, 126388. https://doi.org/10.1016/j.matchemphys.2022.126388

[10] Ahmed, M.A.; Mohamed, A.A. A systematic review of layered double hydroxide-based materials for environmental remediation of heavy metals and dye pollutants. *Inorganic Chemistry Communications*, **2023**, *148*, 110325. https://doi.org/10.1016/j.inoche.2022.110325

[11] Mittal, J. Recent progress in the synthesis of layered double hydroxides and their application for the adsorptive removal of dyes: A review. *Journal of Environmental Management*, **2021**, *295*, 113017. https://doi.org/10.1016/j.jenvman.2021.113017

[12] Liu, L.; Li, S.; An, Y.; Sun, X.; Wu, H.; Li, J.; Chen, X.; Li, H. Hybridization of nanodiamond and CuFe-LDH as heterogeneous photoactivator for visible-light driven photo-fenton reaction: Photocatalytic activity and mechanism. *Catalysts*, **2019**, *9*(2), 118. https://doi.org/10.3390/catal9020118

[13] Mohapatra, L.; Parida, K. A review on the recent progress, challenges and perspective of layered double hydroxides as promising photocatalysts. *Journal of Materials Chemistry A*, **2016**, *4*, 10744-10766. https://doi.org/10.1039/C6TA01668E

[14] Zahedipour, M.; Saien, J.; Pourehie, O. Magnetite CuFe-layered double hydroxide composite in persulfate activation under visible light for degradation of Rhodamine 6G. *Journal of Materials Science: Materials in Electronics*, **2023**, *34*, 598. https://doi.org/10.1007/s10854-023-10032-6

[15] Suppaso, C.; Pongkan, N.; Intachai, S.; Ogawa, M.; Khaorapapong, N. Magnetically recoverable β-Ni(OH)$_2$/γ-Fe$_2$O$_3$/NiFe-LDH composites; Isotherm, thermodynamic, and kinetic studies of synthetic dye adsorption and photocatalytic activity. *Applied Clay Sci*ence, **2021**, *213*, 106115. https://doi.org/10.1016 /j.clay.2021.106115

[16] Intachai, S.; Sumanatrakul, P.; Chaiburi, C.; Pewhom, A.; Nuengmatcha, N.; Khaorapapong. N. Green and facile assembly of LDO, AC, FeOOH and Fe$_3$O$_4$ as multifunctional composite catalyst for efficient biodiesel production and dye degradation. *Fuel*, **2024**, *371*, 132041. https://doi.org/10.1016 /j.fuel.2024.132041

[17] Peng, C.; Yu, Z.; Wu, W.; Li, J.; Wang E. CuFe layered double hydroxide as self-cascade nanoreactor for efficient antibacterial therapy. *ACS Applied Materials & Interfaces*, **2023**, *15*(49), 56678-56688. https://doi.org/10.1021/acsami.3c11757

[18] Vennapoosa, C.S.; Varangane, S.; Gonuguntla, S.; Abraham, B.M.; Ahmadipour, M.; Pal U. S-Scheme ZIF-67/CuFe-LDH heterojunction for high-performance photocatalytic H$_2$ Evolution and CO$_2$ to MeOH production. *Inorganic Chemistry*, **2023**, *62*(40), 16451-16463. https://doi.org/10.1021/acs.inorgchem.3c02126

[19] Khaorapapong, N.; Khumchoo, N.; Ogawa, M. Preparation of copper oxide in smectites. *Applied Clay Science*, **2015**, *104*, 238-244. https://doi.org/10.1016/j.clay.2014.11.038

[20] Intachai, I.; Sumanatrakul, S.; Khaorapapong N. Control of particle growth and enhancement of photoluminescence, adsorption efficiency, and photocatalytic activity for zinc sulfide and cadmium sulfide using CoAl-layered double hydroxide system. *Environmental Science and Pollution Research*, **2023**, *30*, 63230. https://doi.org/10.1007/s11356-023-26778-9

[21] Kansal, S. K.; Ali, A. H.; Kapoor, S. Photocatalytic decolorization of biebrich scarlet dye in aqueous phase using different nanophotocatalysts. *Desalination*, **2010**, *259*(1-3), 147-155. https://doi.org/10.1016 /j.desal.2010.04.017

[22] Ali, O. S.; Al-Mammar, D. E. Adsorption of biebrich scarlet dye onto nano NiO and modified nano NiO: Isotherms, thermodynamic, and kinetic studies. *Journal of Survey in Fisheries Sciences*, **2023**, *10* (3S), 3432-3441.

[23] Begum, S.; Mishra, S.R.; Ahmaruzzaman, M. Fabrication of ZnO–SnO$_2$ nanocomposite and its photocatalytic activity for enhanced degradation of biebrich scarlet. *Environmental Science and Pollution Research*, **2022**, *29*(58), 87347-87360. https://doi.org/10.1007/s11356-022-21851-1